

A homogeneous predictor-corrector algorithm for stochastic nonsymmetric convex conic optimization with discrete support

Baha Alzalg^{1,2,*}, Mohammad Alabedalhadi³

¹Department of Mathematics, The University of Jordan, Amman, Jordan 11942
b.alzalg@ju.edu.jo

²Department of Computer Science and Engineering, The Ohio State University, Columbus, OH 43210

³Department of Applied Science, Balqa Applied University, Ajloun, Jordan 26816
mhm914008s@fgs.ju.edu.jo

Received: 6 November 2021; Accepted: 22 August 2022

Published Online: 27 August 2022

Abstract: We consider a stochastic convex optimization problem over nonsymmetric cones with discrete support. This class of optimization problems has not been studied yet. By using a logarithmically homogeneous self-concordant barrier function, we present a homogeneous predictor-corrector interior-point algorithm for solving stochastic nonsymmetric conic optimization problems. We also derive an iteration bound for the proposed algorithm. Our main result is that we uniquely combine a nonsymmetric algorithm with efficient methods for computing the predictor and corrector directions. Finally, we describe a realistic application and present computational results for instances of the stochastic facility location problem formulated as a stochastic nonsymmetric convex conic optimization problem.

Keywords: Convex optimization, Nonsymmetric programming, Stochastic programming, Predictor-corrector methods, Interior-point methods

AMS Subject classification: 90C15, 90C25, 90C30, 90C51

1. Introduction

Nonsymmetric convex conic optimization [13, 14, 16, 18, 20, 24, 26, 28, 29, 31, 34, 35, 37, 39, 40, 42] is an active research area in mathematical programming. In nonsymmetric programming problems, we minimize a linear function over the intersection of an affine linear manifold with the Cartesian product of nonsymmetric cones (also

* Corresponding Author

known as non-self-scaled cones). Examples of nonsymmetric cones include, but not limited to [16, 20, 24, 26, 29, 35, 37, 39]. The doubly nonnegative cone (the set of positive semidefinite matrices with nonnegative elements), the exponential cone, the power cone, the copositive cone, the completely positive cone, the extended second-order cone, the hyperbolic cone, and the p th-order cone. Therefore, nonsymmetric programming covers a variety of general optimization problems, such as p th-order cone programming [18, 40, 42], copositive programming [13], extended second-order cone programming [28], and hyperbolic programming [31].

Stochastic programming [12] was introduced in the middle of the last century to handle the optimization problems that involve uncertainty in data. There are three basic formulations in stochastic programming. The first formulation is based on Bender's decomposition, which decomposes a stochastic program into stages where, at each stage, variables at preceding stages are considered as constraints so that the subproblem at the current stage is easier to solve. The methods proposed in [2, 4, 5, 8, 9, 15, 41, 43] are based on this formulation. The second formulation is based on the Dantzig-Wolfe decomposition which associates a small program with each scenario and connects all these small programs by the so-called nonanticipativity constraints which, in turn, can be relaxed by the Lagrangian dual. The methods proposed in [27, 32, 44] are based on this formulation. The third formulation is the deterministic equivalence, which is the extensive formulation of a stochastic program that forms an equivalent large one-stage problem containing all constraints and all scenarios. The methods proposed in [3, 6, 7, 11, 19, 21, 25, 36] are based on this formulation.

Despite widespread applications of different classes of nonsymmetric optimization problems [13, 14, 16, 18, 24, 26, 28, 29, 31, 34, 35, 39, 40, 42], they have been studied narrowly in comparison to symmetric optimization problems [5, 33], such as linear programming, second-order cone programming (see for example [1, 22]) and semidefinite programming (see for example [23, 38]). In particular, we emphasize that all the stochastic optimization problems considered in [2–9, 11, 15, 19, 21, 25, 27, 32, 36, 41, 43, 44] are studied over symmetric cones. To the best of our knowledge, there are no studies of interior-point algorithms for stochastic optimization problems over nonsymmetric cones. The main reason for the abundance of stochastic symmetric programming studies and the limitedness of stochastic nonsymmetric programming studies is due to the fact that there is a unifying theory based on Euclidean Jordan algebras that connects all symmetric cones [17, 33]. In the absence of such theory in the case of nonsymmetric cones, one is unable to extend the analysis of some established stochastic interior-point algorithms from symmetric cones to nonsymmetric cones. This makes the study of stochastic nonsymmetric optimization problems more challenging.

In their pioneer work [35], Skajaa and Ye derived a homogeneous interior-point algorithm for the *deterministic* nonsymmetric programming problem. As we mentioned earlier, there are no algorithms that solve the stochastic nonsymmetric programming (SNSP). Inspired by this evident gap in the literature, in this paper, we are interested in developing an interior-point algorithm for solving the two-stage SNSP problem

based on the third formulation, which is the deterministic equivalence, by considering the case in which the event space is finite with K realizations. In fact, the third formulation is found to be more doable than the other two formulations mentioned above for the nonsymmetric setting because the self-concordant analysis is highly involved in the other two formulations which depend very heavily on elements and notions of Euclidean Jordan algebra that are absent in the nonsymmetric case. By utilizing the approach in [35] and exploiting the special structure of the deterministic equivalent formulation, we present a homogeneous predictor-corrector interior-point algorithm that uses a logarithmically homogeneous self-concordant barrier function and solves the two-stage SNSP problem with discrete support. While the analysis in this paper is also influenced, in part, by that in [35] for deterministic nonsymmetric programming, the stochasticity adds a new different dimension of difficulty to our work.

At each iteration of Skajaa and Ye's algorithm [35], the authors used the factorization (Cholesky decomposition) to find the predictor and corrector directions. In [35], the number of factorization steps needed is reduced and the data sparsity is exploited by successfully employing quasi-Newton updating and Runge–Kutta type second-order search direction. In spite of this, we cannot ignore the fact that the factorization step is the most computationally expensive step in Skajaa and Ye's algorithm. The most key part of this paper is describing a method for computing the predictor and corrector directions in the proposed algorithm that exploits the special structures in the deterministic equivalent formulation. This method decomposes into K smaller computations that can be performed in parallel. This is the essence of the proposed algorithm in this paper. We also derive an iteration bound for the algorithm that we develop. The implementation is another key part consisting a realistic application. We present computational experiments for instances of the stochastic facility location problem over nonsymmetric cones. Our computational results show that the proposed algorithm is efficient and is evidently more effective than the existing algorithm in [35] in stochastic environments especially when the number of realizations is very large, which is typically the case in practice. This is due to taking advantage of special deterministic equivalent structures while computing the predictor and corrector directions in this work.

This paper is organized as follows. In the remaining part of this section, we first provide a motivating example for this paper, and then review some definitions and properties that will be used in the subsequent sections. Section 2 is devoted to introducing the SNSP problem, writing its homogeneous model, and identifying the central path associated with the problem. In Sections 3 and 4, the prediction and correction phases for the proposed algorithm are highlighted and discussed. Most notably, Sections 3 and 4 consist the crux of our method for computing the predictor and corrector directions respectively. The homogeneous primal-dual interior-point algorithm is formally stated in Section 5 and its complexity result is also presented there. In Section 6, we present our computational results. Section 7 contains some concluding remarks.

1.1. Motivating example: Stochastic facility location problem

The notations in this part are independent of the other parts of the paper. To model the stochastic facility location problem as our test problem, we use the *power cone* of dimension 3 with parameter $p \geq 1$ defined as

$$C_p^3 := \left\{ x = \begin{pmatrix} x_1 \\ x_2 \\ x_3 \end{pmatrix} \in \mathbb{R}^2 \times \mathbb{R} : x_1^{\frac{1}{p}} x_2^{\frac{p-1}{p}} \geq |x_3| \right\}. \tag{1}$$

It is known that C_p^3 is a nonsymmetric convex cone for any value $p > 1$. Let $t, y_1, y_2, \dots, y_n \in \mathbb{R}$ such that $t = \sum_{i=1}^n y_i$. Note that, for each $i = 1, 2, \dots, n$, we have

$$\begin{aligned} \begin{pmatrix} y_i \\ t \\ x_i \end{pmatrix} \in C_p^3, i = 1, 2, \dots, n &\iff y_i t^{p-1} \geq |x_i|^p, i = 1, 2, \dots, n \\ &\iff t^p = t^{p-1} \sum_{i=1}^n y_i \geq \sum_{i=1}^n |x_i|^p \\ &\iff t \geq \left(\sum_{i=1}^n |x_i|^p \right)^{1/p} = \|x\|_p. \end{aligned} \tag{2}$$

This means that the p^{th} -order cone constraint $t \geq \|x\|_p$, for $x \in \mathbb{R}^n$, can be written as the constraints $(y_i, t, x_i) \in C_p^3, i = 1, 2, \dots, n$, and $e_n^T y = t$, where $y \in \mathbb{R}^n$, and $e_n \in \mathbb{R}^n$ is the vector of all ones. This enables us to formulate a two-stage stochastic facility location problem in \mathbb{R}^{n+1} as the two-stage SNSP problem over three-dimensional power cones.

Assume that we are given f existing fixed facilities with coordinates represented by fixed points, say $a_1, a_2, \dots, a_f \in \mathbb{R}^n$, and r random fixed facilities with coordinates represented by random points, say $b_1(\omega), b_2(\omega), \dots, b_r(\omega) \in \mathbb{R}^n$, whose realizations depend on underlying outcomes ω in an event space Ω with a known probability measure P . In the two-stage stochastic facility location problem, we plan to add a new facility in \mathbb{R}^n among the existing (fixed and random) facilities so that the sum of its weighted distances to the fixed facilities (measured by p_i norms, where $p_i \geq 1$) and the sum of its weighted expected distances to the realizations of the random facilities (measured by q_j norms, where $q_j \geq 1$) are both minimized.

Suppose that, at present time we do not know the realization of r random facilities, and that at some point in the future these realizations become known. Also, suppose that the location of the new facility is to be determined so that the total sum is minimized. This decision needs to be made before the realizations of the random facilities become available. Consequently, when the realization of the random facilities do become available, the location of the new facility that has already been determined, say by the point $x_0 \in \mathbb{R}^n$, may or may not minimize the sum of its weighted expected

distances to the realized random facilities. In order to make the location of the new facility minimizing the total sum of all weighted distances described above, we are allowed to change its location, say to the point $x_0 + x(\omega) \in \mathbb{R}^n$, depending on the realized outcome $\omega \in \Omega$, if necessary. Given this, we are interested in a two-stage stochastic model of the form

$$\min_{x_0} \sum_{i=1}^f \xi_i \|x_0 - a_i\|_{p_i} + \mathbb{E}[Q(x_0, \omega)], \tag{3}$$

where $\mathbb{E}[Q(x_0, \omega)] := \int_{\omega \in \Omega} Q(x_0, \omega) P(d\omega)$, and $Q(x_0, \omega)$ is the minimum value of the problem

$$\min_x \sum_{j=1}^r \zeta_j(\omega) \|x_0 + x(\omega) - b_j(\omega)\|_{q_j}, \tag{4}$$

where $\xi_i \geq 0$ is the weight associated with the distance between the new facility and the i^{th} existing facility for $i = 1, 2, \dots, f$, and $\zeta_j(\omega) \geq 0$ is the weight associated with the expected distance between the new facility and the realization of the j^{th} random facility for $j = 1, 2, \dots, r$.

By the observation that given in (2), we can formulate the two-stage stochastic facility location problem (3, 4) as the following two-stage SNSP problem over power cones with recourse

$$\begin{aligned} \min_{x_0^+, x_0^-, v, u, s} & \sum_{i=1}^f \xi_i u_{i1} + \mathbb{E}[Q(x_0, \omega)] \\ \text{s.t.} & v_i = x_0^+ - x_0^- - a_i, & i = 1, 2, \dots, f, \\ & e_f^T s_i = u_{i1}, u_{i1} = u_{i2} = \dots = u_{in}, & i = 1, 2, \dots, f, \\ & (v_{i\ell}, s_{i\ell}, u_{i\ell}) \in C_{p_i}^3, & i = 1, 2, \dots, f, \ell = 1, 2, \dots, n, \\ & x_0^+, x_0^- \geq 0, \end{aligned} \tag{5}$$

where $\mathbb{E}[Q(x_0, \omega)] := \int_{\omega \in \Omega} Q(x_0, \omega) P(d\omega)$, and $Q(x_0, \omega)$ is the minimum value of the problem

$$\begin{aligned} \min_{x^+, x^-, y, z, t} & \sum_{j=1}^r \zeta_j(\omega) z_{j1}(\omega) \\ \text{s.t.} & y_j(\omega) = x_0^+ - x_0^- + x^+(\omega) - x^-(\omega) - b_j(\omega), & j = 1, 2, \dots, r, \\ & e_r^T t_j(\omega) = z_{j1}(\omega), z_{j1}(\omega) = z_{j2}(\omega) = \dots = z_{jn}(\omega), & j = 1, 2, \dots, r, \\ & (y_{j\ell}(\omega), t_{j\ell}(\omega), z_{j\ell}(\omega)) \in C_{q_j}^3, & j = 1, 2, \dots, r, \ell = 1, 2, \dots, n, \\ & x_0^+, x_0^-, x^+(\omega), x^-(\omega) \geq 0. \end{aligned} \tag{6}$$

Then the two-stage SNSP problem (5, 6) can be formulated as the following SNSP

problem with K scenarios

$$\begin{aligned}
 \min_{\substack{x_0^+, x_0^-, v, u, s \\ x^+, x^-, y, z, t}} & \sum_{i=1}^f \xi_i u_{i1} + \sum_{k=1}^K \sum_{j=1}^r \zeta_j^{(k)} z_{j1}^{(k)} \\
 \text{s.t.} & v_i = x_0^+ - x_0^- - a_i, & i = 1, 2, \dots, f, \\
 & y_j^{(k)} = x_0^+ - x_0^- + x^{(k)+} - x^{(k)-} - b_j^{(k)}, & j = 1, 2, \dots, r, \quad k = 1, \dots, K, \\
 & e_j^+ s_i = u_{i1}, \quad u_{i1} = u_{i2} = \dots = u_{in}, & i = 1, 2, \dots, f, \\
 & e_j^+ t_j^{(k)} = z_{j1}^{(k)}, \quad z_{j1}^{(k)} = z_{j2}^{(k)} = \dots = z_{jn}^{(k)}, & j = 1, 2, \dots, r, \quad k = 1, \dots, K, \\
 & (v_{i\ell}, s_{i\ell}, u_{i\ell}) \in \mathcal{C}_{p_i}^3, & i = 1, 2, \dots, f, \quad \ell = 1, 2, \dots, n, \\
 & \left(y_{j\ell}^{(k)}, t_{j\ell}^{(k)}, z_{j\ell}^{(k)} \right) \in \mathcal{C}_{q_j}^3, & j = 1, \dots, r, \quad \ell = 1, \dots, n, \quad k = 1, \dots, K, \\
 & x_0^+, x_0^-, x^{(k)+}, x^{(k)-} \geq 0, & k = 1, \dots, K.
 \end{aligned} \tag{7}$$

1.2. Preliminaries

Let \mathcal{E} be a finite-dimensional real vector space combined with the dual vector space \mathcal{E}^* and equipped with the scalar product $\langle s, x \rangle$ for $x \in \mathcal{E}$ and $s \in \mathcal{E}^*$. A cone is called *proper* if it is convex, closed, pointed, and solid cone. The *dual cone* of a proper cone $\mathcal{K} \subset \mathcal{E}$ is the cone $\mathcal{K}^* \subset \mathcal{E}^*$ defined as

$$\mathcal{K}^* := \{s \in \mathcal{E}^* : \langle s, x \rangle \geq 0, \forall x \in \mathcal{K}\}.$$

If $\mathcal{K} = \mathcal{K}^*$, we say that \mathcal{K} is *self-dual*. A proper cone is called *homogeneous* if its automorphism group acts transitively on its interior. Proper cones that are both homogeneous and self-dual are called *symmetric cones*. Therefore, *nonsymmetric cones* are the proper cones that lack either homogeneity or self-duality.

Let \mathcal{K} be a proper cone, $\text{int } \mathcal{K}$ denote its interior, and $\text{bd } \mathcal{K}$ denote its boundary. A continuous function $F : \mathcal{K} \rightarrow \mathbb{R} \cup \{\infty\}$ is called a *barrier function* of \mathcal{K} if it satisfies

$$F(x) < \infty \text{ for } x \in \text{int } \mathcal{K}, \text{ and } F(x) = \infty \text{ for } x \in \text{bd } \mathcal{K}.$$

If a barrier $F(x)$ has the form $F(x) := -\ln \phi(x)$ where $\phi(x)$ is continuous function from \mathcal{K} to \mathbb{R}_+ (the set of all non-negative real numbers), then $F(x)$ is said to be a *logarithmic barrier*. A barrier function $F(x)$ is called *self-concordant* if for every $x \in \mathcal{K}$ and $h \in \mathbb{R}^n$, the function $\phi(\alpha) := F(x + \alpha h)$ satisfies the property

$$|\phi(0)'''| \leq 2 \left(\phi(0)'' \right)^{\frac{3}{2}}.$$

A logarithmic barrier function F is called *logarithmically homogeneous* with barrier

parameter v if it satisfies [29]

$$F(tx) = F(x) - v \ln t, \text{ for } x \in \text{int } \mathcal{K} \text{ and } t > 0.$$

A logarithmic barrier function F is called *logarithmically homogeneous self-concordant barrier (LHSCB) function* with barrier parameter v if it is convex, self-concordant, and logarithmically homogeneous with the parameter v .

For example, it is also known [14] that the function

$$F_p(x) := -\ln\left(x_1^{\frac{2}{p}} x_2^{\frac{2(p-1)}{p}} - x_3^2\right) - \frac{p-1}{p} \ln x_1 - \frac{1}{p} \ln x_2$$

is an LHSCB function with parameter 3 for the power cone C_p^3 defined in (1).

Let F be a LHSCB function for the cone \mathcal{K} . Then the function

$$F^*(s) := \max_{x \in \text{int } \mathcal{K}} \{-\langle s, x \rangle - F(x)\}$$

is called *the conjugate function* of F , and it is an LHSCB function for the dual cone \mathcal{K}^* . For $x \in \text{int } \mathcal{K}$ and $s \in \text{int } \mathcal{K}^*$, the LHSCB function F and its conjugate F^* have the following properties [30]:

$$\begin{aligned} -\nabla F(x) &\in \text{int } \mathcal{K}^*, & -\nabla F^*(s) &\in \text{int } \mathcal{K}, \\ \nabla F^*(-\nabla F(x)) &= -x, & \nabla F(-\nabla F^*(s)) &= -s, \\ \nabla^2 F(x)x &= -\nabla F(x), & \langle \nabla F(x), x \rangle &= -\langle \nabla^2 F(x)x, x \rangle = -v, \\ \nabla^2 F(-\nabla F^*(s)) &= \left(\nabla^2 F^*(s)\right)^{-1}, & \nabla^2 F^*(-\nabla F(x)) &= \left(\nabla^2 F(x)\right)^{-1}. \end{aligned}$$

Let $p \in \mathcal{E}, q \in \mathcal{E}^*, x \in \text{int } \mathcal{K}$ and $s \in \text{int } \mathcal{K}^*$. We define the following *local Hessian norms* on \mathcal{K} and \mathcal{K}^* [30]:

$$\begin{aligned} \|p\|_x &:= \left\langle \nabla^2 F(x)p, p \right\rangle^{1/2} = \left\| \left(\nabla^2 F(x)\right)^{1/2} p \right\|, \\ \|q\|_x^* &:= \left\langle q, \left(\nabla^2 F(x)\right)^{-1} q \right\rangle^{1/2} = \left\| \left(\nabla^2 F(x)\right)^{-1/2} q \right\|, \\ \|p\|_s &:= \left\langle \left(\nabla^2 F^*(s)\right)^{-1} p, p \right\rangle^{1/2} = \left\| \left(\nabla^2 F^*(s)\right)^{-1/2} p \right\|, \\ \|q\|_s^* &:= \left\langle q, \left(\nabla^2 F^*(s)\right) q \right\rangle^{1/2} = \left\| \left(\nabla^2 F^*(s)\right)^{1/2} q \right\|, \end{aligned}$$

where $\|\cdot\|$ denotes the Euclidean norm. As shown in [30, 35], for $x \in \text{int } \mathcal{K}$ and $s \in \text{int } \mathcal{K}^*$, we have

$$\|x\|_s = \|s\|_x^* = \|s\|_{-\nabla F(x)}^* \text{ and } \|x\|_x^2 = v.$$

The *Dikin ellipsoid* [10] centered at $x \in \mathcal{K}$ is defined as

$$\mathcal{E}_x := \{p \in \mathcal{E} : \|p - x\|_x \leq 1\},$$

and that centered at $s \in \mathcal{K}^*$ is defined as

$$\mathcal{E}_s^* := \{q \in \mathcal{E}^* : \|q - s\|_s^* \leq 1\}.$$

The Dikin ellipsoids are feasible [10]. That is,

$$\mathcal{E}_x \subseteq \mathcal{K} \text{ for } x \in \text{int } \mathcal{K}, \text{ and } \mathcal{E}_s^* \subseteq \mathcal{K}^* \text{ for } s \in \text{int } \mathcal{K}^*. \quad (8)$$

In Table 1, we summarize the notations that were given in this subsection and will be used throughout the rest of the paper.

Table 1. A table of notations that appear in Subsection 1.2.

Notation	Denotation
\mathbb{R}_+	The set of all non-negative real numbers
\mathbb{R}^n	The space of n -dimensional real vectors
\mathcal{E}	A finite-dimensional real vector space
\mathcal{E}^*	The dual vector space to \mathcal{E}
\mathcal{K}	A proper cone
$\text{int } \mathcal{K}$	The interior of \mathcal{K}
$\text{bd } \mathcal{K}$	The boundary of \mathcal{K}
\mathcal{K}^*	The dual cone of a proper cone
$F(\cdot)$	An LHSCB function for \mathcal{K}
$F^*(\cdot)$	The conjugate function of $F(\cdot)$
$\ \cdot\ $	The Euclidean norm
$\ \cdot\ _x$	Local Hessian norm on \mathcal{K} localized at $x \in \text{int } \mathcal{K}$
$\ \cdot\ _s$	Local Hessian norm on \mathcal{K} localized at $s \in \text{int } \mathcal{K}^*$
$\ \cdot\ _x^*$	Local Hessian norm on \mathcal{K}^* localized at $x \in \text{int } \mathcal{K}$
$\ \cdot\ _s^*$	Local Hessian norm on \mathcal{K}^* localized at $s \in \text{int } \mathcal{K}^*$
\mathcal{E}_x	Dikin ellipsoid centered at $x \in \mathcal{K}$
\mathcal{E}_s^*	Dikin ellipsoid centered at $s \in \mathcal{K}^*$

2. The SNSP problem and its homogeneous model

In this section, we introduce the two-stage SNSP problem, write its corresponding homogeneous model and identify the central path associated with our problem. We define the two-stage SNSP with recourse in primal standard form based on

The dual of (9) is the problem

$$\begin{aligned}
& \max_{y_k, s_k} && h_0^\top y_0 + h_1^\top y_1 + \cdots + h_K^\top y_K \\
& \text{s.t.} && W_0^\top y_0 + B_1^\top y_1 + \cdots + B_K^\top y_K + s_0 = c_0 \\
& && W_1^\top y_1 + s_1 = c_1 \\
& && \ddots \\
& && W_K^\top y_K + s_K = c_K \\
& && s_0 \in \mathcal{K}_1^*, \quad s_1, s_2, \dots, s_K \in \mathcal{K}_2^*,
\end{aligned} \tag{10}$$

where $y_0 \in \mathbb{R}^{m_1}$, $y_k \in \mathbb{R}^{m_2}$, $s_0 \in \mathbb{R}^{n_1}$, and $s_k \in \mathbb{R}^{n_2}$, for $k = 1, 2, \dots, K$, are the decision variables, and \mathcal{K}_1^* and \mathcal{K}_2^* are the dual cones of \mathcal{K}_1 and \mathcal{K}_2 , respectively.

Now, we make the following assumptions.

Assumption 1. Consider the primal-dual pair (9) and (10). The m_1 rows of the matrix W_0 are linearly independent, and, for each $k = 1, 2, \dots, K$, the m_2 rows of the matrix W_k are linearly independent, and the m_2 rows of the matrix B_k are linearly independent.

Assumption 2. Both primal and dual problems are strictly feasible, that is, there exist primal-feasible vectors x_0, x_1, \dots, x_K such that $x_0 \in \text{int } \mathcal{K}_1$ and $x_k \in \text{int } \mathcal{K}_2$, and there exist dual-feasible vectors y_0, y_1, \dots, y_K and s_0, s_1, \dots, s_K such that $s_0 \in \text{int } \mathcal{K}_1^*$ and $s_k \in \text{int } \mathcal{K}_2^*$, for $k = 1, 2, \dots, K$.

Assumption 1 is important to validate the operations described in our upcoming computations. This assumption can be achieved in practice by applying row elimination. Assumption 2 guarantees strong duality for the primal-dual pair (9) and (10).

Let \mathbb{R}_+ denote the set of positive real numbers. The homogeneous model of (9) and (10) is

$$\begin{aligned}
W_0 x_0 - h_0 \tau &= 0; \\
B_k x_0 + W_k x_k - h_k \tau &= 0, k = 0, 1, \dots, K; \\
-W_0^\top y_0 - \sum_{k=1}^K B_k^\top y_k + \tau c_0 - s_0 &= 0; \\
-W_k^\top y_k + \tau c_k - s_k &= 0, k = 0, 1, \dots, K; \\
\sum_{k=0}^K h_k^\top y_k - \sum_{k=0}^K c_k^\top x_k - \lambda &= 0; \\
x_0 \in \mathcal{K}_1, \quad x_k \in \mathcal{K}_2, \quad \tau \in \mathbb{R}_+, & \quad k = 1, 2, \dots, K; \\
s_0 \in \mathcal{K}_1^*, \quad s_k \in \mathcal{K}_2^*, \quad \lambda \in \mathbb{R}_+, & \quad k = 1, 2, \dots, K.
\end{aligned} \tag{11}$$

We can write the system in (11) simply as

$$G \begin{bmatrix} x_0 \\ y_0 \\ x \\ y \\ \tau \end{bmatrix} - \begin{bmatrix} s_0 \\ 0 \\ s \\ 0 \\ \lambda \end{bmatrix} = 0, \quad (12)$$

where

$$x := \begin{bmatrix} x_1 \\ x_2 \\ \vdots \\ x_K \end{bmatrix} \in \mathbb{R}^{K n_2}, y := \begin{bmatrix} y_1 \\ y_2 \\ \vdots \\ y_K \end{bmatrix} \in \mathbb{R}^{K m_2}, s := \begin{bmatrix} s_1 \\ s_2 \\ \vdots \\ s_K \end{bmatrix} \in \mathbb{R}^{K n_2}, \text{ and } G := \begin{bmatrix} 0 & -W_0^T & 0 & -B^T & c_0 \\ W_0 & 0 & 0 & 0 & -h_0 \\ 0 & 0 & 0 & -W^T & c \\ B & 0 & 0 & W & 0 \\ -c_0^T & h_0^T & -c^T & h^T & 0 \end{bmatrix}. \quad (13)$$

Here,

$$c := \begin{bmatrix} c_1 \\ \vdots \\ c_K \end{bmatrix} \in \mathbb{R}^{K n_2}, h := \begin{bmatrix} h_1 \\ \vdots \\ h_K \end{bmatrix} \in \mathbb{R}^{K m_2}, B := \begin{bmatrix} B_1 \\ \vdots \\ B_K \end{bmatrix} \in \mathbb{R}^{K m_1 \times n_1},$$

and

$$W := \text{diag}(W_1, \dots, W_K) \in \mathbb{R}^{K m_2 \times K n_2}.$$

Now, we introduce some notations that will be used in the sequel. We define

$$\begin{aligned} \bar{\mathcal{K}} &:= \mathcal{K}_1 \times \overbrace{\mathcal{K}_2 \times \mathcal{K}_2 \times \dots \times \mathcal{K}_2}^{K\text{-times}} \times \mathbb{R}_+, \\ \bar{\mathcal{K}}^* &:= \mathcal{K}_1^* \times \mathcal{K}_2^* \times \mathcal{K}_2^* \times \dots \times \mathcal{K}_2^* \times \mathbb{R}_+, \\ \mathcal{F} &:= \bar{\mathcal{K}} \times \bar{\mathcal{K}}^* \times \mathbb{R}^{m_1 + K m_2}. \end{aligned}$$

Besides the vectors x, y and s defined in (13), we define

$$\bar{x} := \begin{bmatrix} x_0 \\ x \\ \tau \end{bmatrix}, \bar{s} := \begin{bmatrix} s_0 \\ s \\ \lambda \end{bmatrix}, \bar{y} := \begin{bmatrix} y_0 \\ y \end{bmatrix}, \text{ and } z := \begin{bmatrix} \bar{x} \\ \bar{s} \\ \bar{y} \end{bmatrix}.$$

Associated with each z , we also define

$$\hat{z} := \begin{bmatrix} x_0 \\ y_0 \\ x \\ y \\ \tau \end{bmatrix}, \text{ and } \check{z} := \begin{bmatrix} s_0 \\ 0 \\ s \\ 0 \\ \lambda \end{bmatrix}. \quad (14)$$

Note that, using (14), equation (12) can be written as

$$G\hat{z} - \check{z} = 0, \tag{15}$$

where the matrix G is defined in (13). Note also that G is skew-symmetric (i.e., $G^T = -G$). The proof of the following lemma is essentially based on the skew-symmetry of the constraint system of our homogeneous model.

Lemma 1. *The following optimization problem is self-dual.*

$$\begin{aligned} \min \quad & 0 \\ \text{s.t.} \quad & G\hat{z} - \check{z} = 0 \\ & z \in \mathcal{F}. \end{aligned}$$

Lemma 1 is important in the subsequent developments in the paper, because it tells us that a primal-dual interior-point algorithm can be applied to solve the homogeneous model (15) when $z \in \mathcal{F}$. Like all interior-point methods, in our algorithm we track the central path to approach a solution.

Let F_1 be a LHSCB function with barrier parameter v_1 for the cone \mathcal{K}_1 , and F_2 be a LHSCB function with barrier parameter v_2 for the cone \mathcal{K}_2 , then the function

$$\bar{F}(\bar{x}) := F_1(x_0) + \sum_{k=1}^K F_2(x_k) - \ln \tau$$

is a LHSCB function for the cone $\bar{\mathcal{K}}$ with barrier parameter $v_1 + Kv_2 + 1$. This immediately follows by noting that

$$\begin{aligned} \bar{F}(t\bar{x}) &= F_1(tx_0) + \sum_{k=1}^K F_2(tx_k) - \ln(t\tau) \\ &= F_1(x_0) - v_1 \ln t + \sum_{k=1}^K (F_2(x_k) - v_2 \ln t) - \ln t - \ln \tau \\ &= \left(F_1(x_0) + \sum_{k=1}^K F_2(x_k) - \ln \tau \right) - (v_1 + Kv_2 + 1) \ln t \\ &= \bar{F}(\bar{x}) - (v_1 + Kv_2 + 1) \ln t. \end{aligned}$$

Following the notions in Section 2, we use the following norms for $p \in \bar{\mathcal{K}}$ and $q \in \bar{\mathcal{K}}^*$:

$$\|p\|_{\bar{x}} := \left\| (\nabla^2 \bar{F}(\bar{x}))^{1/2} p \right\| \quad \text{and} \quad \|q\|_{\bar{x}}^* := \left\| (\nabla^2 \bar{F}(\bar{x}))^{-1/2} q \right\|.$$

We define the *complementary gap* by

$$\mu(z) := \frac{\bar{x}^T \bar{s}}{v_1 + Kv_2 + 1} \quad \text{for } z \in \mathcal{F}. \quad (16)$$

Our algorithm is initialized with $z^0 := (\bar{x}^0, \bar{s}^0, \bar{y}^0) \in \mathcal{F}$. Let $\mu^0 := \mu(z^0)$. The *central path* of the homogeneous model (12), which is parametrized by $\gamma \in [0, 1]$, is defined by the points $z_\gamma := (\bar{x}_\gamma, \bar{s}_\gamma, \bar{y}_\gamma)$ that satisfy

$$\begin{aligned} G\hat{z}_\gamma - \check{z}_\gamma &= \gamma(G\hat{z}^0 - \check{z}^0), \\ \psi(\bar{x}_\gamma, \bar{s}_\gamma, \gamma\mu^0) &= 0, \end{aligned} \quad (17)$$

where

$$\psi(\bar{x}, \bar{s}, t) := \bar{s} + t\nabla\bar{F}(\bar{x}), \quad \text{for } \bar{x} \in \bar{\mathcal{K}}, \bar{s} \in \bar{\mathcal{K}}^*, \text{ and a scalar } t. \quad (18)$$

For a fixed parameter $\eta \in [0, 1]$, we define the *neighborhood* of the central path as follows

$$\mathcal{N}(\eta) := \{z \in \mathcal{F} : \|\psi(\bar{x}, \bar{s}, \mu(z))\|_{\bar{x}}^* \leq \eta \mu(z)\}.$$

Starting from the initial point z^0 (at $\gamma = 1$), the central path approaches a solution of (15) as γ decreases to zero. This guarantees the convergence of the central path to the solution of the original problem.

3. An efficient method for computing the predictor direction

In this section, we discuss the prediction phase of the algorithm. We particularly describe an efficient method for computing the predictor direction and then discuss the termination of the prediction process.

The *predictor direction* is the direction d_z tangent to the central path. This direction can be determined by differentiating the system (17) with respect to γ .

Using (18), the second equation in (17) can be written as

$$\bar{s}_\gamma + \gamma\mu^0\nabla\bar{F}(\bar{x}_\gamma) = 0, \quad \text{or equivalently } \mu^0\nabla\bar{F}(\bar{x}_\gamma) = -\gamma^{-1}\bar{s}_\gamma. \quad (19)$$

Let $d_{\bar{x}_\gamma} := \partial\bar{x}_\gamma/\partial\gamma$ and similarly for all other variables. By differentiating the left-hand side equation in (19) with respect to γ , we get

$$d_{\bar{s}_\gamma} + \gamma\mu^0\nabla^2\bar{F}(\bar{x}_\gamma)d_{\bar{x}_\gamma} + \mu^0\nabla\bar{F}(\bar{x}_\gamma) = 0,$$

which, by using the right-hand side equation in (19) and putting $\mu(z) := \gamma\mu^0$ (here μ^0

is obtained from (16) by setting $(\bar{x}, \bar{s}) = (\bar{x}^0, \bar{s}^0)$, can be written as

$$d_{\bar{s}, \gamma} + \mu(z) \nabla^2 \bar{F}(\bar{x}_\gamma) d_{\bar{x}, \gamma} = \gamma^{-1} \bar{s}_\gamma. \quad (20)$$

Using (15) and (20), after rescaling the later by $-\gamma$, we can conclude that the differentiation of the system (17) with respect to γ is the system

$$\begin{aligned} Gd_z - d_z &= -(G\hat{z} - \check{z}), \\ d_{\bar{s}} + \mu(z) \nabla^2 F(\bar{x}) d_{\bar{x}} &= -\bar{s}. \end{aligned} \quad (21)$$

Note that, for the sake of simplicity, we dropped the argument γ . Thus, the predictor direction d_z is determined by solving the system (21). In fact, we have

$$\begin{aligned} \bar{s}^\top d_{\bar{x}} + \bar{x}^\top d_{\bar{s}} + \bar{x}^\top \bar{s} &= \psi(z)^\top d_{\bar{x}}, \\ (\bar{x} + d_{\bar{x}})^\top (\bar{s} + d_{\bar{s}}) &= 0, \\ d_{\bar{x}}^\top d_{\bar{s}} &= -\psi(z)^\top d_{\bar{x}}, \end{aligned} \quad (22)$$

where the first equation follows from the second equation in (21) and the definition of $\psi(\cdot)$, the second equation follows from reordering the first equation in (21) and multiplying the result by $(\bar{y} + d_{\bar{y}}, \bar{x} + d_{\bar{x}})$, and the third one follows from expanding the second and using the first.

We now describe a method for computing the predictor direction. As we have seen, the predictor direction d_z is determined by solving the system (21). This system can be written as

$$\begin{aligned} W_0 d_{x_0} - h_0 d_\tau &= -r_1, \\ B_k d_{x_0} + W_k d_{x_k} - h_k d_\tau &= -r_{2k}, \\ -W_0^\top d_{y_0} - \sum_{k=1}^K B_k^\top d_{y_k} + d_\tau c_0 - d_{s_0} &= -r_3, \\ -W_k^\top d_{y_k} + d_\tau c_k - d_{s_k} &= -r_{4k}, \\ \sum_{k=0}^K h_k^\top d_{y_k} - \sum_{k=0}^K c_k^\top d_{x_k} - d_\lambda &= -r_5, \\ \lambda d_\tau + \tau d_\lambda &= -\tau \lambda, \\ d_{s_0} + \mu \nabla^2 F_1(x_0) d_{x_0} &= -s_0, \\ d_{s_k} + \mu \nabla^2 F_2(x_k) d_{x_k} &= -s_k, \end{aligned} \quad (23)$$

where $k = 1, 2, \dots, K$ and

$$\begin{aligned} r_1 &:= W_0 x_0 - h_0 \tau, & r_{4k} &:= -W_k^\top y_k + \tau c_k - s_k, \\ r_{2k} &:= B_k x_0 + W_k x_k - h_k \tau, & r_5 &:= \sum_{k=0}^K h_k^\top y_k - \sum_{k=0}^K c_k^\top x_k - \lambda. \\ r_3 &:= -W_0^\top y_0 - \sum_{k=1}^K B_k^\top y_k + \tau c_0 - s_0, \end{aligned}$$

Using the last equation of (23), we get

$$d_{s_k} = -\mu \nabla^2 F_2(x_k) d_{x_k} - s_k \quad (24)$$

for $k = 1, 2, \dots, K$. By substituting this equation into the fifth equation of (23) we can write d_{x_k} as

$$d_{x_k} = \left(\mu \nabla^2 F_2(x_k) \right)^{-1} \left(-r_{4k} + W_k^\top d_{y_k} - d_\tau c_k - s_k \right) \quad (25)$$

for $k = 1, 2, \dots, K$. We now substitute (25) into the second equation of (23) to get

$$M_k d_{y_k} - q_k d_\tau + B_k d_{x_0} - n_k = -r_{2k}$$

where

$$\begin{aligned} M_k &:= W_k (\mu \nabla^2 F_2(x_k))^{-1} W_k^\top, \\ q_k &:= W_k (\mu \nabla^2 F_2(x_k))^{-1} c_k + h_k, \\ n_k &:= W_k (\mu \nabla^2 F_2(x_k))^{-1} (r_{4k} + s_k), \end{aligned}$$

for $k = 1, 2, \dots, K$. This gives

$$d_{y_k} = -M_k^{-1} (B_k d_{x_0} - q_k d_\tau - n_k + r_{2k}). \quad (26)$$

Using the seventh equation of (23), we obtain

$$d_{s_0} = -\mu \nabla^2 F_1(x_0) d_{x_0} - s_0. \quad (27)$$

Using this equation and (26) in the third equation of (23), we get

$$-W_0^\top d_{y_0} + \left(\sum_{k=1}^K B_k^\top M_k^{-1} B_k \right) d_{x_0} - \left(\sum_{k=1}^K B_k^\top q_k \right) d_\tau - \sum_{k=1}^K B_k^\top n_k + d_\tau c_0 + \mu \nabla^2 F_1(x_0) d_{x_0} + s_0 = -r_3.$$

Thus, we can write d_{x_0} as

$$d_{x_0} = M_0^{-1} W_0^\top d_{y_0} - N d_\tau + U, \quad (28)$$

where

$$\begin{aligned} M_0 &:= \mu \nabla^2 F_1(x_0) + \sum_{k=1}^K B_k^\top M_k^{-1} B_k, \\ N &:= M_0^{-1} \left(c_0 - \sum_{k=1}^K B_k^\top q_k \right), \\ U &:= M_0^{-1} \left(\sum_{k=1}^K B_k^\top n_k - r_3 + s_0 \right). \end{aligned}$$

We now substitute (28) into the first equation of (23) to obtain

$$W_0 (M_0^{-1} W_0^\top d_{y_0} - N d_\tau + U) - h_0 d_\tau = -r_1.$$

Using the above equation, d_{y_0} can be expressed as

$$d_{y_0} = \alpha_0 d_\tau + \beta_0, \quad (29)$$

where

$$\begin{aligned}\alpha_0 &:= \left(W_0 M_0^{-1} W_0^T\right)^{-1} (W_0 N + h_0), \\ \beta_0 &:= -\left(W_0 M_0^{-1} W_0^T\right)^{-1} (W_0 U + r_1).\end{aligned}$$

Now the next step is backward substituting to obtain $d_{x_0}, d_{y_k}, d_{x_k}$ and then d_τ . First, we substitute (29) in (28) to get

$$d_{x_0} = M_0^{-1} W_0^T (\alpha_0 d_\tau + \beta_0) - N d_\tau + U.$$

So, d_{x_0} can be written as

$$d_{x_0} = \psi_0 d_\tau + \phi_0, \quad (30)$$

where

$$\begin{aligned}\psi_0 &:= M_0^{-1} W_0^T \alpha_0 - N, \\ \phi_0 &:= M_0^{-1} W_0^T \beta_0 - U.\end{aligned}$$

Substituting (30) in (26), we obtain

$$d_{y_k} = -M_k^{-1} B_k (\psi_0 d_\tau + \phi_0) + q_k d_\tau + n_k.$$

From this equation, one can write d_{y_k} as

$$d_{y_k} = \alpha_k d_\tau + \beta_k, \quad (31)$$

where

$$\begin{aligned}\alpha_k &:= -M_k^{-1} B_k \psi_0 + q_k, \\ \beta_k &:= -M_k^{-1} B_k \phi_0 + n_k,\end{aligned}$$

for $k = 1, 2, \dots, K$. Also, we substitute (31) in (25) to get

$$d_{x_k} = \left(\mu \nabla^2 F_2(x_k)\right)^{-1} \left(-r_{4k} + W_k^T (\alpha_k d_\tau + \beta_k) - d_\tau c_k - s_k\right).$$

Hence, d_{x_k} can be written as

$$d_{x_k} = \psi_k d_\tau + \phi_k, \quad (32)$$

where

$$\begin{aligned}\psi_k &:= \left(\mu \nabla^2 F_2(x_k)\right)^{-1} \left(W_k^T \alpha_k - c_k\right), \\ \phi_k &:= \left(\mu \nabla^2 F_2(x_k)\right)^{-1} \left(W_k^T \beta_k - r_{4k} - s_k\right),\end{aligned}$$

for $k = 1, 2, \dots, K$. Now, we substitute (29), (30), (31), and (32) into the fifth equation

of (23) to obtain

$$\sum_{k=0}^K h_k^\top (\alpha_k d_\tau + \beta_k) - \sum_{k=0}^K c_k^\top (\psi_k d_\tau + \phi_k) - \frac{1}{\tau} (-\lambda \tau - d_\tau \lambda) = -r_5.$$

Thus, d_τ is given by

$$d_\tau = \frac{-\sum_{k=0}^K (h_k^\top \beta_k - c_k^\top \phi_k) - (\lambda + r_5)}{\tau \sum_{k=0}^K (h_k^\top \alpha_k - c_k^\top \psi_k) + \lambda}. \quad (33)$$

Finally, using the sixth equation of (23), d_λ is given by

$$d_\lambda = -\frac{\lambda}{\tau} d_\tau - \lambda. \quad (34)$$

We now discuss the convergence of the prediction process. In this process, z denotes the starting point and z^+ denotes the point after the prediction step. Defining

$$z^+ := (\bar{x}^+, \bar{s}^+, \bar{y}^+) := (\bar{x} + \alpha d_{\bar{x}}, \bar{s} + \alpha d_{\bar{s}}, \bar{y} + \alpha d_{\bar{y}}) = z + \alpha d_z \quad \text{and} \quad \mu^+ := \mu(z^+).$$

Similarly, we also define $\hat{z}^+ := \hat{z} + \alpha d_{\hat{z}}$ and $\check{z}^+ := \check{z} + \alpha d_{\check{z}}$. Then, the predictor direction d_z satisfies the system

$$\begin{aligned} G\hat{z}^+ - \check{z}^+ &= (1 - \alpha)(G\hat{z} - \check{z}), \\ \mu(z^+) &= (1 - \alpha)\mu(z) + (1 - \alpha)\alpha \frac{\psi(z)^\top d_{\bar{x}}}{v_1 + Kv_2 + 1}, \end{aligned} \quad (35)$$

where the first equation is nothing more than applying elementary linear algebra to the first equation of (17), and the second follows directly from the complementary gap and using (22).

One can prove that, if $z \in \mathcal{N}(\eta)$, then the following bounds for \bar{s} , $d_{\bar{s}}$ and $d_{\bar{x}}$ can indeed be obtained:

$$\begin{aligned} \|\bar{s}\|_{\bar{x}}^* &\leq \mu \sqrt{\eta^2 + v_1 + Kv_2 + 1}, \\ \|d_{\bar{x}}\|_{\bar{x}} &\leq k_{\bar{x}} := \eta + \sqrt{\eta^2 + v_1 + Kv_2 + 1}, \\ \|d_{\bar{s}}\|_{\bar{x}}^* &\leq k_{\bar{s}} \mu, \quad \text{where } k_{\bar{s}} := k_{\bar{x}} + \sqrt{\eta^2 + v_1 + Kv_2 + 1 + k_{\bar{x}}^2}. \end{aligned} \quad (36)$$

In addition, for $\eta \leq 1/6$, the following bound for $\psi^+ := \psi(\bar{x}^+, \bar{s}^+, \mu(z^+))$ can also be obtained:

$$\|\psi^+\|_{\bar{x}}^* \leq 2\eta\mu^+. \quad (37)$$

In the following lemma, the big Omega notation " $\alpha = (1/\sqrt{v_1 + Kv_2})$ " means that

there exist a positive (possibly small) constant c_0 and a natural number v_0 such that $\alpha \geq c_0 / \sqrt{v_1 + Kv_2}$ for all v_1 and v_2 having $v_1 + Kv_2 \geq v_0(1 + K)$.

Lemma 2. *Let $z \in \mathcal{N}(\eta)$. Then*

(1) *we can choose $\alpha = \Omega(1 / \sqrt{v_1 + Kv_2})$ so that $z^+ \in \mathcal{F}$,*

(2) *if $\eta \leq 1/6$, then we can choose $\alpha = \Omega(1 / \sqrt{v_1 + Kv_2})$ so that $z^+ \in \mathcal{N}(2\eta)$.*

Proof Letting $\alpha_1 := 1/k_{\bar{x}} = \Omega(1 / \sqrt{v_1 + Kv_2})$ and using the second inequality in (36), then for any $\alpha \leq \alpha_1$ we get

$$\|\bar{x} - \bar{x}^+\|_{\bar{x}} = \|\bar{x} - (\bar{x} + \alpha d_{\bar{x}})\|_{\bar{x}} = \alpha \|d_{\bar{x}}\|_{\bar{x}} \leq \alpha k_{\bar{x}} \leq 1,$$

and hence by (8), we have $\bar{x}^+ \in \bar{\mathcal{K}}$.

Similarly, letting $\alpha_2 := (1 - \eta)/k_{\bar{s}} = \Omega(1 / \sqrt{v_1 + Kv_2})$ and using the third inequality in (36), then for any $\alpha \leq \alpha_2$ we get

$$\begin{aligned} \frac{1}{\mu} \|\bar{s}^+ + \mu \nabla F(\bar{x})\|_{-\nabla F(\bar{x})}^* &= \frac{1}{\mu} \|\bar{s} + \alpha d_{\bar{s}} + \mu \nabla F(\bar{x})\|_{-\nabla F(\bar{x})}^* \\ &= \frac{1}{\mu} \|\psi + \alpha d_{\bar{s}}\|_{-\nabla F(\bar{x})}^* \\ &\leq \frac{1}{\mu} \|\psi\|_{-\nabla F(\bar{x})}^* + \frac{1}{\mu} \alpha \|d_{\bar{s}}\|_{-\nabla F(\bar{x})}^* \\ &\leq \eta + \alpha k_{\bar{s}} \\ &\leq 1. \end{aligned}$$

Hence, using the fact that $-\mu \nabla F(\bar{x}) \in \bar{\mathcal{K}}^*$ and using (8), we have $(1/\mu)\bar{s}^+ \in \bar{\mathcal{K}}^*$, and hence $\bar{s}^+ \in \bar{\mathcal{K}}^*$. The fact that $\bar{x}^+ \in \bar{\mathcal{K}}$ and that $\bar{s}^+ \in \bar{\mathcal{K}}^*$ demonstrate the feasibility of z^+ . The first item is established. The second item follows directly from (37). The proof is complete. \square

4. Computation of the corrector direction

In this section, we discuss the correction phase of the algorithm. In analogy to the method presented in Section 3, this section presents the summary of a similar method applied to compute the corrector direction. We also discuss the termination of the correction process.

In the *correction phase*, our focus is to find a new point $z = (\bar{x}, \bar{s}, \bar{y})$ closer to the central path (in the sense that $z \in \mathcal{N}(\eta)$) satisfying the same constraints as z^+ , i.e., $G\hat{z} - \hat{z} = G\hat{z}^+ - \hat{z}^+$. This leads us to apply Newton's method to the system

$$\begin{aligned} G\hat{z} - \hat{z} &= G\hat{z}^+ - \hat{z}^+, \\ \psi(\bar{x}, \bar{s}, \mu(z)) &= 0. \end{aligned} \tag{38}$$

Let

$$\delta_{\bar{x}} := \begin{bmatrix} \delta_{x_0} \\ \delta_x \\ \delta_\tau \end{bmatrix}, \quad \delta_{\bar{s}} := \begin{bmatrix} \delta_{s_0} \\ \delta_s \\ \delta_\lambda \end{bmatrix}, \quad \delta_{\bar{y}} := \begin{bmatrix} \delta_{y_0} \\ \delta_y \end{bmatrix}, \quad \text{then } \delta_z := \begin{bmatrix} \delta_{\bar{x}} \\ \delta_{\bar{s}} \\ \delta_{\bar{y}} \end{bmatrix}$$

is the Newton step for (38). Following our notations in a previous section, we also let

$$\delta_z := \begin{bmatrix} \delta_{x_0} \\ \delta_{y_0} \\ \delta_x \\ \delta_y \\ \delta_\tau \end{bmatrix} \quad \text{and} \quad \delta_z := \begin{bmatrix} \delta_{s_0} \\ 0 \\ \delta_s \\ 0 \\ \delta_\lambda \end{bmatrix}.$$

Note that the Newton step δ_z is determined by solving the system

$$\begin{aligned} G\delta_z - \delta_z &= 0, \\ \delta_{\bar{s}} + \mu(z) \left(\nabla^2 F(\bar{x}) \right) \delta_{\bar{x}} &= -\psi(\bar{x}, \bar{s}, \mu(z)). \end{aligned} \quad (39)$$

Applying a similar method as that in Section 3 for the predictor direction, we can show that the corrector direction δ_z is given by

$$\begin{aligned} \delta_{x_0} &= \widetilde{\psi}_0 \delta_\tau + \widetilde{\phi}_0, \\ \delta_{x_k} &= \widetilde{\psi}_k \delta_\tau + \widetilde{\phi}_k, \\ \delta_{s_0} &= -\mu \nabla^2 F_1(x_0) \delta_{x_0} - \widetilde{r}_2, \\ \delta_{s_k} &= -\mu \nabla^2 F_2(x_k) \delta_{x_k} - \widetilde{r}_{3k}, \\ \delta_{y_0} &= \widetilde{\alpha}_0 \delta_\tau + \widetilde{\beta}_0, \\ \delta_{y_k} &= \widetilde{\alpha}_k \delta_\tau + \widetilde{\beta}_k, \\ \delta_\tau &= \frac{-\sum_{k=0}^K (h_k^\top \widetilde{\beta}_k - c_k^\top \widetilde{\phi}_k) - \widetilde{r}_1}{\tau \sum_{k=0}^K (h_k^\top \widetilde{\alpha}_k - c_k^\top \widetilde{\psi}_k) + \lambda}, \\ \delta_\lambda &= -\frac{1}{\tau} (\widetilde{r}_1 + \lambda \delta_\tau), \end{aligned} \quad (40)$$

where $k = 1, 2, \dots, K$ and

$$\begin{aligned} \widetilde{r}_1 &:= \tau \lambda - \mu, & \widetilde{N} &:= \widetilde{M}_0^{-1} (c_0 - \sum_{k=1}^K B_k^\top \widetilde{q}_k) \\ \widetilde{r}_2 &:= s_0 + \mu \nabla F_1(x_0), & \widetilde{U} &:= \widetilde{M}_0^{-1} \left(\sum_{k=1}^K B_k^\top \widetilde{n}_k + \widetilde{r}_2 \right) \\ \widetilde{r}_{3k} &:= s_k + \mu \nabla F_2(x_k), & \widetilde{\psi}_0 &:= \widetilde{M}_0^{-1} W_0^\top \widetilde{\alpha}_0 - \widetilde{N}, \\ \widetilde{\alpha}_0 &:= (W_0 \widetilde{M}_0^{-1} W_0^\top)^{-1} (W_0 \widetilde{N} + h_0), & \widetilde{\psi}_k &:= (\mu \nabla^2 F_2(x_k))^{-1} (W_k^\top \widetilde{\alpha}_k - c_k), \\ \widetilde{\alpha}_k &:= -\widetilde{M}_k^{-1} B_k \widetilde{\psi}_0 + \widetilde{q}_k, & \widetilde{\phi}_0 &:= \widetilde{M}_0^{-1} W_0^\top \widetilde{\beta}_0 - \widetilde{U}, \\ \widetilde{\beta}_0 &:= -(W_0 \widetilde{M}_0^{-1} W_0^\top)^{-1} (W_0 \widetilde{U}), & \widetilde{\phi}_k &:= (\mu \nabla^2 F_2(x_k))^{-1} (W_k^\top \widetilde{\beta}_k - \widetilde{r}_{3k}), \\ \widetilde{\beta}_k &:= -\widetilde{M}_k^{-1} B_k \widetilde{\phi}_0 + \widetilde{n}_k, & \widetilde{q}_k &:= \widetilde{M}_k^{-1} (W_k (\mu \nabla^2 F_2(x_k))^{-1} c_k + h_k), \\ \widetilde{M}_0 &:= \mu \nabla^2 F_1(x_0) + \sum_{k=1}^K B_k^\top \widetilde{M}_k^{-1} B_k, & \widetilde{n}_k &:= \widetilde{M}_k^{-1} (W_k (\mu \nabla^2 F_2(x_k))^{-1} \widetilde{r}_{3k}). \\ \widetilde{M}_k &:= W_k (\mu \nabla^2 F_2(x_k))^{-1} W_k^\top, \end{aligned}$$

To discuss the convergence of the correction process, we present the following lemma which demonstrates that the termination of this phase is quick.

Lemma 3. *If $\eta \leq 1/6$, then the correction process (41) terminates in at most two steps.*

Proof In the correction process, we start with $z = z^+$ and solve (39) for $z = z^+$, then we apply

$$z = z^{++} := (\bar{x}^{++}, \bar{s}^{++}, \bar{y}^{++}) := (\bar{x}^+ + \hat{\alpha}\delta_{\bar{x}^+}, \bar{s}^+ + \hat{\alpha}\delta_{\bar{s}^+}, \bar{y}^+ + \hat{\alpha}\delta_{\bar{y}^+}) = z^+ + \hat{\alpha}\delta_{z^+}, \quad (41)$$

repeatedly until the condition $\|\psi(\bar{x}, \bar{s}, \mu(z))\|_{\bar{x}}^* \leq \eta\mu(z)$ is fulfilled. Assuming that $\|\psi(\bar{x}, \bar{s}, \mu(z))\|_{\bar{x}}^* \leq \beta\mu(z)$, it is not hard to see that the following bounds for $\delta_{\bar{s}}$ and $\delta_{\bar{x}}$ can indeed be obtained:

$$\|\delta_{\bar{x}}\|_{\bar{x}} \leq \beta \quad \text{and} \quad \|\delta_{\bar{s}}\|_{\bar{x}}^* \leq \beta\mu. \quad (42)$$

In addition, by applying the correction process (41) twice and recursively using (42) twice, we can also see that, for $\hat{\alpha} \leq 1/84$, $v_1 + Kv_2 \geq 1$ and $\beta \leq 2\eta \leq 1/3$, the following bound for $\psi^{++} := \psi(\bar{x}^{++}, \bar{s}^{++}, \mu(z^{++}))$ can be obtained:

$$\|\psi^{++}\|_{\bar{x}}^* \leq \frac{\beta\mu^{++}}{2} \leq \eta\mu^{++},$$

where $\mu^{++} := \mu(z^{++})$. This means that $z^{++} \in \mathcal{N}(\eta)$ after at most two steps. □

5. The homogeneous predictor-corrector algorithm and its complexity

In this section, we present our algorithm for solving the SNSP problem and its complexity result. We formally state a homogeneous predictor-corrector interior-point algorithm for SNSP in Algorithm 1.

Algorithm 1. Stochastic Nonsymmetric Predictor-Corrector Algorithm

begin algorithm

1 **initialize** LHSCB function \bar{F} , initial point $z := (x_0, x, \tau, s_0, s, \lambda, y_0, y)$, η, β

ensure: $z \in \mathcal{F} \cap \mathcal{N}(\eta)$, $0 < \eta \leq \beta < 1$

2 set $\hat{z} := (x_0, y_0, x, s, \tau)$, $\check{z} := (s_0, 0, s, 0, \lambda)$, $\bar{x} := (x_0, x, \tau)$, $\bar{s} := (s_0, s, \lambda)$, $\bar{y} := (y_0, y)$, $\mu := \mu(z)$

3 **while** a stopping criterion is not satisfied **do**

begin prediction

4 compute the predictor direction d_z using (24), (27), (29) – (34)

5 choose largest α so that $z + \alpha d_z \in \mathcal{F} \cap \mathcal{N}(\beta)$

6 set $z := z + \alpha d_z$

7 update $\hat{z}, \check{z}, \bar{x}, \bar{s}, \bar{y}, \mu$

end prediction

begin correction

8 **while** $z \notin \mathcal{F} \cap \mathcal{N}(\eta)$ **do**

9 compute the corrector direction δ_z using (40)

10 choose $\hat{\alpha}$ to approximately minimize $\|\psi\|_x^*$ along δ_z

11 set $z := z + \hat{\alpha} \delta_z$

12 update $\hat{z}, \check{z}, \bar{x}, \bar{s}, \bar{y}, \mu$

13 **end while**

end correction

14 **end while**

end algorithm

Now, we state and prove the complexity result for Algorithm 1.

Theorem 1. *Algorithm 1 terminates with a point $z = (\bar{x}, \bar{s}, \bar{y})$ that satisfies*

$$\|G\hat{z} - \check{z}\| \leq \epsilon \|G\check{z}^0 - \check{z}^0\| \quad \text{and} \quad \mu(z) \leq \epsilon \mu(z^0)$$

in no more than $\mathcal{O}(\sqrt{v_1 + Kv_2} \ln(1/\epsilon))$ iterations.

Proof From the first equation in (35), we have $G\hat{z}^+ - \check{z}^+ = (1 - \alpha)(G\hat{z} - \check{z})$. Now, we can choose

$$\alpha := \Omega\left(\frac{1}{\sqrt{v_1 + Kv_2}}\right)$$

and see that the difference $G\hat{z} - \check{z}$ decreases geometrically with a rate of $(1 - \Omega(1/\sqrt{v_1 + Kv_2}))$, which implies that $\|G\hat{z} - \check{z}\| \leq \epsilon \|G\hat{z}^0 - \check{z}^0\|$ in

$$\mathcal{O}\left(\sqrt{v_1 + Kv_2} \ln\left(\frac{1}{\epsilon}\right)\right)$$

iterations.

Now, we show that the same result is true for $\mu(z)$ as well. Following our notations in Section 3, let z be the starting point and z^+ be the point after the prediction step. Let also z^{++1} be the point after applying the first correction step starting in z^+ and z^{++2} be the point after applying the second correction step starting in z^+ .

Note that

$$\begin{aligned} \mu(z^+) &\leq (1 - \alpha)\mu(z) + \alpha(1 - \alpha) \frac{\psi^\top d_{\bar{x}}}{v_1 + Kv_2} && \text{(using the second equality in (35))} \\ &\leq (1 - \alpha)\mu(z) + \alpha(1 - \alpha) \frac{\|\psi\|_{\bar{x}}^* \|d_{\bar{x}}\|_{\bar{x}}}{v_1 + Kv_2} && \text{(using Cauchy-Schwarz inequality)} \\ &\leq (1 - \alpha)\mu(z) + \alpha(1 - \alpha) \frac{\|\psi\|_{\bar{x}}^* k_{\bar{x}}}{v_1 + Kv_2} && \text{(using the second inequality in (36))} \\ &\leq (1 - \alpha)\mu(z) + \alpha(1 - \alpha) \frac{2\mu(z) \eta k_{\bar{x}}}{v_1 + Kv_2} && \text{(using the inequality in (37))} \\ &\leq \mu(z)(1 - \alpha) \left(1 + \frac{2\alpha\eta k_{\bar{x}}}{v_1 + Kv_2}\right). \end{aligned}$$

Therefore

$$\mu(z^+) = \mu(z) \left(1 - \Omega\left(\frac{1}{\sqrt{v_1 + Kv_2}}\right)\right). \quad (43)$$

After left-multiplying the first equation in (39) by $(\delta_y, \delta_{\bar{x}})^\top$, we have $\delta_{\bar{x}}^\top \delta_s = 0$. As a result, from the second equation in (39), we also have

$$\bar{x}^{+\top} \delta_s = \mu(z^+) \delta_{\bar{x}}^\top \nabla F(\bar{x}^+) = \delta_{\bar{x}}^\top \psi^+ - \delta_{\bar{x}}^\top \bar{s}^+. \quad (44)$$

It immediately follows that

$$\begin{aligned} (v_1 + Kv_2)\mu(z^{++1}) &= (\bar{x}^+ + \hat{\alpha}\delta_{\bar{x}})^\top (\bar{s}^+ + \hat{\alpha}\delta_s) && \text{(from the complementary gap (16))} \\ &= \bar{x}^{+\top} \bar{s}^+ + \hat{\alpha}\delta_{\bar{x}}^\top \psi^+ + \hat{\alpha}^2 \delta_{\bar{x}}^\top \delta_s && \text{(using (44))} \\ &= \bar{x}^{+\top} \bar{s}^+ + \hat{\alpha}\delta_{\bar{x}}^\top \psi^+ && \text{(using } \delta_{\bar{x}}^\top \delta_s = 0) \\ &\leq (v_1 + Kv_2)\mu(z^+) + \hat{\alpha}\beta^2 \mu(z^+) && \text{(from the complementary gap (16))} \\ &= (v_1 + Kv_2)\mu(z^+) \left(1 + \frac{\hat{\alpha}\beta^2}{v_1 + Kv_2}\right). \end{aligned}$$

Hence, we have

$$\mu(z^{++1}) \leq \mu(z^+) \left(1 + \frac{\hat{\alpha}\beta^2}{v_1 + Kv_2} \right). \tag{45}$$

Consequently, we have that

$$\begin{aligned} \mu(z^{++2}) &\leq \mu(z^+) \left(1 + \frac{\hat{\alpha}\beta^2}{v_1 + Kv_2} \right)^2 && \text{(applying (45) recursively twice)} \\ &\leq \mu(z) \left(1 - \Omega \left(\frac{1}{\sqrt{v_1 + Kv_2}} \right) \right) \left(1 + \frac{\hat{\alpha}\beta^2}{v_1 + Kv_2} \right)^2 && \text{(using the inequality in (43))} \\ &= \mu(z) \left(1 - \Omega \left(\frac{1}{\sqrt{v_1 + Kv_2}} \right) \right). \end{aligned}$$

This means that $\mu(z)$ is decreased geometrically with rate of $\left(1 - \Omega \left(1/\sqrt{v_1 + Kv_2} \right) \right)$. This implies that $\mu(z) \leq \epsilon\mu(z^0)$ in

$$\mathcal{O} \left(\sqrt{v_1 + Kv_2} \ln \left(\frac{1}{\epsilon} \right) \right)$$

iterations. The proof is complete. □

6. Experimental implementation

In this section, we present computational experiments that demonstrate the efficiency of Algorithm 1. We also prove the effectiveness of Algorithm 1 by comparing its performance with that of the existing algorithm in [35]. To obtain our numerical experiments, we used MATLAB Version R2013b on Windows 7 Ultimate, which carried out on a PC with Intel(R) Core(TM) i5-4210U CPU at 2.40 GHz and 6 GB of physical memory.

Test problems We implement Algorithm 1 to solve the SNSP problem (7). In the test problem, we consider instances of the stochastic facility location problem which was formulated as an SNSP problem in Subsection 1.1. We run Algorithm 1 on random instances of K scenarios of the SNSP problem (7), where the dimension of the problem takes the values $n = 2, 10, 20$, the number of fixed facilities takes the values $f = 3, 15, 30$, the number of random facilities takes the values $r = 4, 20, 40$, and the number of realizations takes the values $K = 5, 25, 50$, with an associated probability $p_k = \frac{1}{K}$ for each $k = 1, 2, \dots, K$. The parameters of Algorithm 1 are given as $\epsilon = 10^{-6}$, $\beta = 0.80$ and $\eta = 0.50$. For each quadruple (n, f, r, K) , we generated 20 instances each with a_i and $b_j^{(k)}$ chosen at random from the standard normal distribution. In the implementation, we choose f different p_i 's as the maximum of 1.0 and a sample from a normal distribution with mean 2.0 and variance 0.25. Similarly, we also choose r different q_j 's as the maximum of 1.0

and a sample from a normal distribution with mean 2.0 and variance 0.25. We choose the distance weights ξ_i and $\zeta_j^{(k)}$ randomly from a uniform distribution on $[0, 1]$.

Table 2. Numerical results for the stochastic facility location problem (7).

Problem size and number of realizations							Results form SNPCA		Results form DNPCA	
n	f	r	\bar{p}	\bar{q}	K	v	Iter	CPU(s)	Iter	CPU(s)
2	3	4	1.07	1.04	5	184	14.3	0.25041	15.1	0.29835
2	3	4	0.94	1.06	25	824	18.1	1.01985	26.7	2.21643
2	3	4	1.07	0.98	50	1624	27.9	6.32981	51.3	8.11162
2	15	20	1.07	1.01	5	920	30.3	1.76529	28.2	1.71271
2	15	20	1.05	1.07	25	4120	37.8	9.88731	45.9	14.62010
2	15	20	0.96	1.03	50	8120	48.8	13.11827	68.5	19.90165
2	30	40	1.01	1.09	5	1840	44.6	9.05843	47.0	12.41687
2	30	40	0.92	0.99	25	8240	54.5	17.44904	59.8	22.15439
2	30	40	1.09	1.00	50	16240	61.0	28.10194	90.4	40.80400
10	3	4	1.00	0.92	5	736	42.2	15.55627	42.9	17.52498
10	3	4	1.06	1.09	25	3296	62.4	31.84620	73.1	37.14924
10	3	4	1.03	1.04	50	6496	68.6	43.13579	94.3	58.66244
10	15	20	0.91	1.05	5	3680	63.4	37.02110	66.7	43.58121
10	15	20	1.06	1.08	25	16480	76.6	46.18438	83.8	51.74138
10	15	20	1.06	1.02	50	32480	87.6	55.04640	112.4	72.31422
10	30	40	1.03	0.97	5	7360	81.9	52.34811	87.3	56.42374
10	30	40	1.00	1.08	25	32960	91.1	60.51378	103.1	68.74881
10	30	40	0.97	1.01	50	64960	91.0	71.65248	122.5	83.41410
20	3	4	0.98	0.93	5	1426	93.5	57.00981	91.4	55.98791
20	3	4	1.07	1.00	25	6386	104.8	66.78106	109.5	72.21410
20	3	4	1.09	1.07	50	12586	109.5	72.21497	137.1	86.32811
20	15	20	0.91	1.03	5	7130	99.3	64.98124	107.3	69.15060
20	15	20	1.00	1.09	25	31930	111.3	73.66091	124.6	84.12749
20	15	20	1.04	1.05	50	62930	128.1	81.31459	154.9	96.20021
20	30	40	0.99	1.00	5	14260	119.4	66.08199	124.0	72.81074
20	30	40	1.09	1.03	25	63860	126.5	89.64892	142.3	109.62481
20	30	40	0.97	1.01	50	125860	144.5	103.7713	217.7	149.02400

Presentation of numerical results The numerical results of Algorithm 1 are summarized in Table 2. In our numerical results, “Iter” denotes the number of iterations taken to obtain the optimal solution, and “CPU(s)” denotes the CPU time (in seconds) required to obtain the optimal solution. Note that the values of “Iter” and “CPU(s)” are the average of 20 runs for each quadruple (n, f, r, K) . The column labeled “ \bar{p} ” shows the number $(1/f) \sum_{i=1}^f p_i$ averaged over the 20 instances, and the column la-

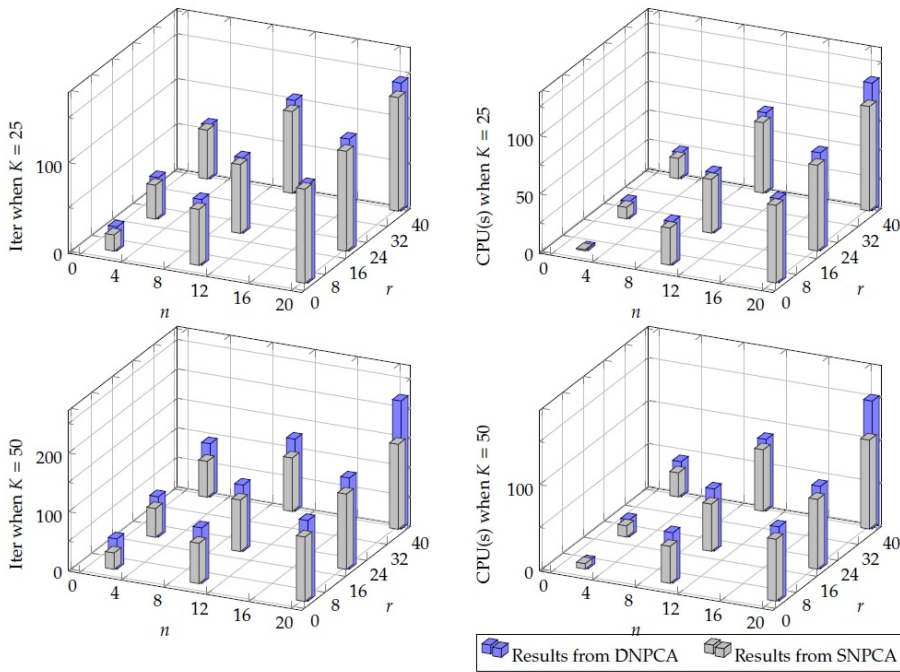


Figure 1. The numerical results for the stochastic facility location problem (when $K = 25, 50$) are translated into three-dimensional bar charts for comparison purposes.

beled “ \bar{q} ” shows the number $(1/r) \sum_{i=1}^r q_j$ averaged over the 20 instances. So, all the numbers in the columns labeled “ \bar{p} ” and “ \bar{q} ” should be close to 1.0. The column labeled “Results from SNPCHA” shows the numerical results obtained by Algorithm 1, namely, the stochastic nonsymmetric predictor-corrector algorithm.

We point out that similar, but simpler, numerical examples have been reported in [35, Section 5] and [14, Chapter 4] to test the performance of deterministic nonsymmetric primal-dual predictor-corrector methods in [35, Algorithm 2] and [14, Algorithm 5] respectively. Because Problem (7) can be viewed as a large (one-stage) deterministic problem containing all constraints and all scenarios, for comparison purpose, we also implement the existing algorithm in [35] for solving Problem (7). The column labeled “Results from DNPCHA” shows the numerical results by the deterministic nonsymmetric predictor-corrector algorithm proposed in [35]. The optimal solutions are reached by using Algorithm 1 because all problem instances are feasible by construction.

Discussion of numerical results The computational results in Table 2 show that Algorithm 1 is efficient overall. In our results, over all instances, we found that Algorithm 1 uses in the region 11-65 iterations and the CPU time never exceeds 29

when $n = 2$, it uses in the region 38-93 iterations and the CPU time never exceeds 73 when $n = 10$, and that it uses in the region 90-152 iterations and the CPU time never exceeds 108 when $n = 20$.

Using the methods described in Sections 3 and 4 for computing the predictor and corrector directions, we are overall able to produce computational results in Table 2 that affirm that Algorithm 1 is more effective than the existing algorithm in [35] in a stochastic environment with a large number of realizations K , which is typically the case in practice. This can be explicitly seen when $K = 25$ and $K = 50$. To be cautious, except for a few of problems, we can say that for the facility location problems, Algorithm 1 compares somewhat unfavorably to the existing algorithm in [35] when K is small, but it compares favorably to the existing algorithm in [35] when K is large, typically greater than 20. In Figure 1, we show the numerical results in Table 2 for $K = 25, 50$.

It is obvious from Figure 1 that Algorithm 1 has superiority over the existing algorithm in [35] in the stochastic environments, and both in terms of iterations and CPU time. This is despite of the data sparsity is exploited in [35] by successfully employing quasi-Newton updating and Runge–Kutta type second-order search direction to reduce the number of factorization steps needed. The main reason for the superiority of Algorithm 1 is that the factorization step is the most computationally expensive step while computing the predictor and corrector directions in [35]. On the other hand, the methods described in Sections 3 and 4 decompose into K smaller computations that are performed in parallel.

Summary of numerical results To conclude and sum up, after working on the stochastic facility location problem with K scenarios that we described, modeled, and implemented above as our SNSP test problem, the obtained computational results indicate that, overall, Algorithm 1 performs very well in practice.

7. Concluding remarks

In this paper, we have studied and solved two-stage stochastic convex optimization problems where both the first- and second-stage problems are nonsymmetric conic optimization problems. The problem that we tackled in this work is interesting, and, to the best of our knowledge, there are no previous studies in the literature addressing this important class of stochastic conic optimization problems. We have presented a homogeneous predictor-corrector primal-dual interior-point algorithm for this optimization problem with finite event space. The algorithm consists of efficient methods for computing the predictor and corrector directions which are established by exploiting the special structure of the resulting extensive formulation. We have also presented the complexity of the proposed algorithm and have shown its convergence. Concerning the implementation issues for the proposed algorithm, we have seen from our computational results that the algorithm is efficiently implemented for instances of the stochastic facility location problem formulated

as SNSP problems. As we exploit special structures while computing predictor and corrector directions, computational results demonstrate also the superiority of the proposed algorithm for stochastic environments over the existing one in [35]. Another point that worths noting (not shown in our numerical results, but can be known by inspection) is that Algorithm 1 is generic in the sense that its performance depends a lot on the type of the underlying problem. For instance, the choice of the parameters of our algorithm, such as ϵ , β , and η , depends a lot on the type of the underlying nonsymmetric cone. Future work is devoted to develop interior-point methods for solving linearly constrained stochastic convex programming over nonsymmetric cones.

Conflict of interest. The authors declare that they have no conflict of interest.

References

- [1] F. Alizadeh and D. Goldfarb, *Second-order cone programming*, Math. Program. Ser. B **95** (2003), no. 1, 3–51.
- [2] B. Alzalg, *Decomposition-based interior point methods for stochastic quadratic second-order cone programming*, Appl. Math. Comput. **249** (2014), 1–18.
- [3] ———, *Homogeneous self-dual algorithms for stochastic second-order cone programming*, J. Optim. Theory Appl. **163** (2014), no. 1, 148–164.
- [4] ———, *Volumetric barrier decomposition algorithms for stochastic quadratic second-order cone programming*, App. Math. Comput. **265** (2015), 494–508.
- [5] B. Alzalg and K.A. Ariyawansa, *Logarithmic barrier decomposition-based interior point methods for stochastic symmetric programming*, J. Math. Anal. Appl. **409** (2014), no. 2, 973–995.
- [6] B. Alzalg, K. Badarneh, and A. Ababneh, *An infeasible interior-point algorithm for stochastic second-order cone optimization*, J. Optim. Theory Appl. **181** (2019), no. 1, 324–346.
- [7] B. Alzalg, F. Maggioni, and S. Vitali, *Homogeneous self-dual methods for symmetric cones under uncertainty*, Far East J. Math. Sc. **99** (2016), no. 11, 1603–1778.
- [8] K. Ariyawansa and Y. Zhu, *A class of polynomial volumetric barrier decomposition algorithms for stochastic semidefinite programming*, Math Comput. **80** (2011), no. 275, 1639–1661.
- [9] K.A. Ariyawansa and Y. Zhu, *A class of volumetric barrier decomposition algorithms for stochastic quadratic programming*, Appl. Math. Comput. **186** (2007), no. 2, 1683–1693.
- [10] A. Ben-Tal and A. Nemirovski, *Lectures on modern convex optimization: analysis, algorithms, and engineering applications*, SIAM, Philadelphia, 2001.
- [11] J.R. Birge and D.F. Holmes, *Efficient solution of two-stage stochastic linear programs using interior point methods*, Comp. Optim. Appl. **1** (1992), no. 3, 245–276.

- [12] J.R. Birge and F. Louveaux, *Introduction to Stochastic Programming*, Springer Science & Business Media, 2011.
- [13] I.M. Bomze, *Copositive optimization—recent developments and applications*, European J. Oper. Res. **216** (2012), no. 3, 509–520.
- [14] P.R. Chares, *Algorithms for unsymmetric cone optimization and an implementation for problems with the exponential cone*, Ph.D. thesis, Uni. Catholique de Louvain, 2009.
- [15] G.-M. Cho, *Log-barrier method for two-stage quadratic stochastic programming*, Appl. Math. Comput. **164** (2005), no. 1, 45–69.
- [16] J. Dahl and E.D. Andersen, *A primal-dual interior-point algorithm for nonsymmetric exponential-cone optimization*, Math. Program. **194** (2022), no. 1, 341–370.
- [17] J. Faraut, *Analysis on symmetric cones*, Oxford University Press, Oxford, UK, 1994.
- [18] F. Glineur and T. Terlaky, *Conic formulation for l_p -norm optimization*, J. Optim. Theory Appl. **122** (2004), no. 2, 285–307.
- [19] M. Hegland, M.R. Osborne, and J. Sun, *Parallel interior point schemes for solving multistage convex programming*, Ann. Oper. Res. **108** (2001), no. 1, 75–85.
- [20] R. Hildebrand, *On the algebraic structure of the copositive cone*, Optim. Lett. **14** (2020), no. 8, 2007–2019.
- [21] S. Jin and Y. Ariyawansa, K.A. and Zhu, *Homogeneous self-dual algorithms for stochastic semidefinite programming*, J. Optim. Theory Appl. **155** (2012), no. 3, 1073–1083.
- [22] B. Kheirfam, *A corrector-predictor path-following method for second-order cone optimization*, Int. J. Comput. Math. **93** (2016), no. 12, 2064–2078.
- [23] B. Kheirfam, N. Osmanpour, and M. Keyanpour, *An arc-search infeasible interior-point method for semidefinite optimization with the negative infinity neighborhood*, Nume. Algorithms **88** (2021), no. 1, 143–163.
- [24] Y. Lu, C.-Y. Yang, J.-S. Chen, and H.-D. Qi, *The decompositions with respect to two core non-symmetric cones*, J. Global Optim. **76** (2020), no. 1, 155–188.
- [25] I.J. Lustig, J.M. Mulvey, and T.J. Carpenter, *Formulating two-stage stochastic programs for interior point methods*, Oper. Res. **39** (1991), no. 5, 757–770.
- [26] Y. Matsukawa and A. Yoshise, *A primal barrier function phase I algorithm for non-symmetric conic optimization problems*, Japan J. Indust. Appl. Math. **29** (2012), no. 3, 499–517.
- [27] J.M. Mulvey and A. Ruszczyński, *A new scenario decomposition method for large-scale stochastic optimization*, Oper. Res. **43** (1995), no. 3, 477–490.
- [28] S.Z. Németh and G. Zhang, *Extended lorentz cones and mixed complementarity problems*, J. Global Optim. **62** (2015), no. 3, 443–457.
- [29] Y.E. Nesterov, *Towards non-symmetric conic optimization*, Optim. Method Softw. **27** (2012), no. 4-5, 893–917.
- [30] Y.E. Nesterov and M.J. Todd, *Self-scaled barriers and interior-point methods for convex programming*, Math. Oper. Res. **22** (1997), no. 1, 1–42.
- [31] J. Renegar, *Hyperbolic programs, and their derivative relaxations*, Found. Comput. Math. **6** (2005), 59–79.
- [32] R.T. Rockafellar and R.J.B. Wets, *Scenarios and policy aggregation in optimization*

- under uncertainty*, Math. Oper. Res. **16** (1991), no. 1, 119–147.
- [33] S.H. Schmieta and F. Alizadeh, *Extension of primal-dual interior point algorithms to symmetric cones*, Math. Program. Ser. A **96** (2003), no. 3, 409–438.
- [34] S.A. Serrano, *Cones and interior-point algorithms for structured convex optimization involving powers and exponentials*, Ph.D. thesis, Stanford University, 2015.
- [35] A. Skajaa and Y. Ye, *A homogeneous interior-point algorithm for nonsymmetric convex conic optimization*, Math. Program. Ser. A **150** (2015), no. 2, 391–422.
- [36] J. Sun and X. Liu, *Scenario formulation of stochastic linear programs and the homogeneous self-dual interior-point method*, INFORMS J. Comput. **18** (2006), no. 4, 444–454.
- [37] Y. Sun, S. Pan, and S. Bi, *Metric subregularity and/or calmness of the normal cone mapping to the p -order conic constraint system*, Optim. Lett. **13** (2019), no. 5, 1095–1110.
- [38] M.J. Todd, *Semidefinite optimization*, Acta Numer. **10** (2001), 515–560.
- [39] L. Tunçel, *Generalization of primal–dual interior-point methods to convex optimization problems in conic form*, Found. Comput. Math. **1** (2001), no. 3, 229–254.
- [40] Alexander V. and Pavlo A.K., *Polyhedral approximations in p -order cone programming*, Optim. Methods Softw. **29** (2014), no. 6, 1210–1237.
- [41] R.M. Van Slyke and R. Wets, *L -shaped linear programs with applications to optimal control and stochastic programming*, SIAM J. Applied Math. **17** (1969), no. 4, 638–663.
- [42] A. Vinel and P. Krokmal, *On valid inequalities for mixed integer p -order cone programming*, J. Optim. Theory Appl. **160** (2014), no. 2, 439–456.
- [43] G. Zhao, *A log-barrier method with Benders decomposition for solving two-stage stochastic linear programs*, Math. Program. Ser. A **90** (2001), no. 3, 507–536.
- [44] ———, *A Lagrangian dual method with self-concordant barriers for multi-stage stochastic convex programming*, Math. Program. **102** (2005), no. 1, 1–24.